Protein Expression and Purification **16,** 236–242 (1999)
Article ID prep.1999.1070, available online at http://www.idealibrary.com on IDEAL®

Purification, Characterization, and Crystallization of the Distal BRCT Domain of the Human XRCC1 DNA Repair Protein

Kevin Thornton, Michael Forstner, M. Richard Shen,[1] Mary G. West, Bernhard Rupp, and Michael P. Thelen[2]

Molecular and Structural Biology Division, Biology and Biotechnology Research Program, Lawrence Livermore National Laboratory, Livermore, California 94550

Received November 2, 1998, and in revised form March 10, 1999

The XRCC1 DNA repair protein contains two regions of approximately 100 amino acids each that share homology with the BRCT (BRCA1 carboxyl terminus) domain superfamily. These two regions of XRCC1 have been shown to interact independently with DNA ligase III and poly(ADP-ribose)polymerase as part of a mechanism involved in the repair of DNA single-strand breaks. To understand how these BRCT regions specify protein–protein interactions and contribute to DNA repair function, we have overexpressed and purified the distal BRCT domain of XRCC1 with the goal of structure determination. The cDNA encoding this BRCT region (X1BRCTb) was inserted into the pET29 bacterial expression vector; the polypeptide was expressed in mostly soluble form and then purified by anion-exchange and gel filtration chromatography. Crystallization screening with the purified material resulted in the formation of large bipyramidal crystals. Crystals formed within several hours at room temperature from salt solutions of ammonium sulfate. Crystals diffract to ~2.85 Å and were found to be in space group $P4_12_12$ (or its enantiomorph $P4_32_12$) with unit cell dimensions $a = 100.43$ Å, $c = 105.62$ Å. Crystals of similar character have also been obtained after incorporation of selenomethionine during expression of the protein. Efforts are now under way to determine the molecular structure of the X1BRCTb domain. These studies are likely to give insight into the interaction between XRCC1 and DNA ligase III and into general structural features of BRCT domains that exist in many other proteins.

[1] Current address: Myriad Genetics Laboratories, Inc., 320 Wakara Way, Salt Lake City, UT 84108.

[2] To whom correspondence should be addressed at Biology and Biotechnology Research Program, Lawrence Livermore National Laboratory, P.O. Box 808, L-452 Livermore, CA 94551. Fax: (925) 422-2282. E-mail: mthelen@llnl.gov.

Key Words: **BRCT domain; XRCC1; DNA ligase III; single-strand break repair; protein–protein interaction; crystallography.**

The BRCT (BRCA1 carboxyl terminus) domain is a widely duplicated sequence module recently identified by homology shared between more than 40 proteins, many of which are central to DNA repair and cell cycle control processes (1, 2). The domain superfamily was initially defined by conservation within a tandemly repeated region of 100 residues found in the human breast cancer-associated protein BRCA1 and several disparate proteins (3). One member of this superfamily is XRCC1 (X-ray repair cross-complementing 1), a mammalian protein which functions in the repair of base damage and DNA single-strand breaks (4, 5). The repair function of XRCC1 is dependent on the specific association between its C-terminal region and the C-terminal region of DNA ligase IIIα (Lig IIIα) (6, 7), both of which contain distinct BRCT domains. Interaction of XRCC1 with Lig IIIα is dependent on a 20 amino acid block within the BRCT module of XRCC1 (8). Another BRCT domain identified in the midsection of XRCC1 interacts with two discreet regions of poly(ADP-ribose)-polymerase (PARP), one of which has BRCT homology (9). We use the nomenclature "X1BRCTa" and "X1BRCTb" to indicate the respective proximal and distal interacting domains within XRCC1 (5) (see Fig. 1).

Homology based on conventional pairwise or multiple alignment search algorithms was insufficient to define this superfamily. Sequence alignments were augmented by predictive methods, such as protein secondary structure and hydrophobicity pattern matching, in order to identify the BRCT domain within pro-

1046-5928/99

teins of this superfamily (1, 2). As in BRCA1, the BRCT domain is often found in tandem repeats at the C-terminus of proteins, but also as a single copy and elsewhere in the protein. Although computational tools predicted a common set of features consisting of two α-helices surrounded by β-strands, these structural elements and the molecular structure of any BRCT domain are yet to be determined. It is considered likely that BRCT will be an independent structural unit that is autonomously folding (1).

The observed sequence similarity of a BRCT module within a set of proteins that function in DNA transcription, repair, or replication suggests that BRCT may link the functions of these proteins to the cell cycle checkpoint machinery (1, 2). Although the function of this domain is not understood, it does appear likely that protein–protein interactions are specified by BRCT modules. This is known to be the case in the specific associations between BRCT domains of the *Schizosaccharomyces pombe* proteins Crb2 and Cut5 (11), as well as the human proteins XRCC4 and DNA ligase IV (12), XRCC1 (X1BRCTb) and DNA ligase III (7,8), and XRCC1 (X1BRCTa) and PARP (9). A BRCT-containing protein may also interact specifically with proteins lacking a BRCT domain. Such is the case with the 53BP1, in which a carboxy terminal fragment, consisting mostly of two BRCT domains, binds specifically with p53 (13) and also TopBP1, which contains eight BRCT domains and interacts with DNA topoisomerase IIβ (14). BRCT function is implicated in early onset breast and ovarian cancers: loss of the two BRCT domains in mutant alleles of *BRCA-1* is sufficient to cause these diseases (15). The structure of this domain will directly impact the understanding of many BRCT-containing proteins, including human BRCA1, 53BP1, ECT2, TdT, TopBP1, DNA ligase III, DNA ligase IV, XRCC1, XRCC4, and PARP; *Saccharomyces cerevisiae* RAD9, REV1, RAP1, and DBP11; and *S. pombe* rad4/cut5 and crb2.

To determine the structure of the BRCT module, toward understanding its apparent role in DNA repair or associated cellular functions, we overexpressed, purified, and crystallized the distal BRCT domain, X1BRCTb, of the human XRCC1 protein. Crystals obtained thus far diffract X rays to ~2.85 Å and have been used to collect initial data.

MATERIALS AND METHODS

Cloning. To isolate the putative structural domain X1BRCTb (residues 538–633 of XRCC1), the plasmid pcD2EX containing the human *XRCC1* cDNA (4) was used to amplify the region between nucleotides 1597 to 1902 by polymerase chain reaction (PCR). Deoxyribonucleotide primers (obtained from Genset, Inc.) used for amplification were forward, 5′TATACATATGGATCTGCCAGTCCCTGAGC3′; and reverse, 5′AGTGCGGCCGCTCAGGCTTGCGGCACCAC3′. The underlined nucleotides of the forward and reverse primers denote the *Nde*I and *Eag*I sites, respectively, used in cloning the 306-bp product. PCR using Pfu polymerase (Stratagene) consisted of 94°C (5 min), followed by 25 cycles of 94°C denaturation (30 s), 55°C annealing (45 s), and 72°C extension (45 s), and was completed by a 72°C (7 min) extension. The product was cloned using standard techniques (16) into the pET-29a(+) vector (Novagen, Inc.) using the *Nde*I and *Eag*I sites in the plasmid. NovaBlue bacteria (Novagen) were transformed to kanamycin resistance, plasmid DNA was isolated from transformants, and the entire sequence of the insert and flanking regions was verified by DNA sequencing. The resulting construct, pXB1.2, contains the 3′ region of the *XRCC1* cDNA inserted after the ribosomal binding site of pET29, so that the ORF begins at a nonnative codon for Met and terminates at the native stop codon of *XRCC1*.

X1BRCTb production and purification. For protein expression, pXB1.2 was transformed into *Escherichia coli* strains BL21(DE3) and B834(DE3) (Novagen). Typically, an overnight culture was diluted 1 to 100 in LB medium containing 25 μg/mL kanamycin. These cultures were grown at 37°C until the A_{600} value was 0.6–0.7. Protein expression was induced by addition of IPTG to a final concentration of 0.4mM. The cultures were then grown for 5 h at 37°C and harvested by centrifugation at 4000*g* for 20 min at 4°C. The supernatant was removed and the pelleted cells frozen at −20°C. The cells were lysed by resuspending the cells in 20 mM bis[2-hydroxyethyl]iminotris[hydroxymethyl]-methane (Bis–Tris), pH 6.0, 100 mM NaCl, 10 mM DTT and passing the suspension through a French press twice at 20,000 psi. The lysate was centrifuged for 20 min at 12,000*g*, and the supernatant (corresponding to 0.5 L of culture) was loaded onto a 20 mL Macro-Prep Q ion-exchange column (Bio-Rad, Inc.). The column was then washed with 5 column vol of 90% Buffer A (20 mM Bis–Tris, pH 6.0) and 10% Buffer B (20 mM Bis–Tris, pH 6.0, 1 M NaCl) followed by a 15-mL wash with 15% Buffer B. The protein was eluted with a linear gradient of 15% Buffer B to 30% Buffer B over 3 column vol followed by 30% Buffer B for 2 column vol. Fractions containing X1BRCTb as identified by SDS-PAGE and immunodetection were combined (Fraction I) and diluted with Buffer A to approximately three times the volume of the lysate sample loaded and then reloaded onto the Q20 column. X1BRCTb was eluted with 40% Buffer B. Fractions containing X1BRCTb were pooled (Fraction II), concentrated to less than 10 mL by dialysis centrifugation (Centriprep-3; Amicon), and then loaded onto a preparative Superdex-75 column (Amersham Pharmacia Bio-

tech; 2.5 × 100 cm; 2.5 mL/min) that was equilibrated in 50 mM K-phosphate buffer, pH 7.0, 500 mM KCl. Fractions from this column containing X1BRCTb were combined (Fraction III), concentrated, and exchanged into 10 mM Na-phosphate buffer, pH 7.0, using an Amicon 8MC micro-ultrafiltration system (YM3 membrane, Amicon). Protein content was determined by the Bio-Rad microassay protocol. Purity was assessed by analyzing the stained polyacrylamide gel photograph image, using 1D image analysis software (Eastman Kodak Co.) to capture the image and calculate band intensities.

For estimation of X1BRCTb molecular mass under solution conditions used for purification, a parallel run of the Superdex-75 column was performed with the following standards: aprotinin (6500), cytochrome *c* (12,400), carbonic anhydrase (29,000), and bovine albumin (66,000). The resulting correlation coefficient (R^2) for the standards was 0.998.

Production of selenomethionine protein. For incorporation of selenomethionine (Se-Met) into X1BRCTb for crystallographic multiwavelength anomalous dispersion (MAD) phasing experiments, the B834(DE3)/pXB1.2 strain was inoculated from a 40-mL seed culture into M9 medium, 25 μg/mL kanamycin, at 37°C until the A_{600} value was 0.6–1.0. The medium was then changed by resuspending harvested cells in a modified, Met-free LeMaster's minimal medium (17) containing 25 μg/mL kanamycin, 5 mM Se-Met (Sigma), and 0.4 mM IPTG to induce expression. After 3 h the cells were harvested and stored at −80°C. The purification procedure was identical to that of the nonlabeled protein except that all chromatography buffers contained 1 mM dithiothreitol.

SDS–polyacryamide gel electrophoresis. All SDS–PAGE protein samples were prepared for electrophoresis using a 2× Tris–glycine sample buffer (Novex) containing dithiothreitol. The samples were heated for 2–3 min at 90°C prior to electrophoresis and then separated on a 4–20% polyacrylamide Tris–glycine gel (Bio-Rad Laboratories) and stained with Coomassie blue R-250 (Sigma).

Immunodetection. After electrophoretic separation, proteins were transferred to a nitrocellulose membrane using a transfer apparatus (Bio-Rad) at 20 V overnight. Protein molecular mass markers (Novex) were detected on the membrane using Ponceau-S (Sigma) staining before or after immunodetection procedures. X1BRCTb was then detected using an affinity-purified mouse polyclonal antibody raised against human XRCC1 (5), followed by a secondary anti-mouse IgG, peroxidase-linked species-specific F(ab′) fragment (Amersham Life Sciences). Lig III proteins were detected similarly, using a rabbit polyclonal antibody raised against Lig IIIβ, a generous gift from Dr. Alan Tomkinson, and followed by the appropriate secondary antibody (Bio-Rad). The immunoblot was developed by incubation with chemiluminescence reagent according to the manufacturer (Pierce) and subsequent exposure to Kodak autoradiographic X-OMAT film.

Domain:protein interactions. X1BRCTb:Lig III interactions studies were carried out using the bulk GST purification module (Amersham Pharmacia Biotech). Glutathione *S*-transferase (GST) fusion constructs of Lig IIIα and β were generously provided by Dr. Alan Tomkinson. *Escherichia coli* BL21 cells were transformed to both kanamycin and ampicillin resistance with pXB1.2 and a pGEX plasmid containing GST–Lig IIIα, GST–Lig IIIβ, or no insert (parental GST fusion protein alone). Bacteria selected to contain both plasmids were then induced to coexpress X1BRCTb and one of the GST proteins by addition of IPTG to 0.4 mM. X1BRCTb was expressed equally well in all three GST protein backgrounds (data not shown). For GST affinity capture, glutathione–Sepharose 4B was preequilibrated with Binding Buffer [50 mM Hepes (pH 7.9), 100 mM NaCl, 1 mM dithiothreitol, 0.1 mM EDTA, 10% glycerol] containing 0.1% Nonidet P-40 and 2% dried milk, as described (6). Induced bacterial cells were lysed by sonicating in Binding Buffer and then centrifuged at 12,000*g* for 10 min at 4°C. After adding Nonidet P-40 to 0.1%, a 50% slurry of GST–Sepharose was added to the sonicate at 1/25 the sonicate volume and mixed by gentle shaking for 30 min at room temperature. The Sepharose was washed three times with Binding Buffer containing 0.1% Nonidet P-40. Proteins remaining bound to GST–Sepharose were separated by SDS–PAGE after incubating samples for 10 min at 70°C in 1× SDS sample buffer (1/25 the sonicate volume). X1BRCTb, GST–Lig III, and GST were all visible by both Coomassie blue staining and immunoblotting. Normalization of samples was achieved by comparing the stained GST fusion proteins using the 1D image analysis software.

Circular dichroism. Spectra were acquired on a Jasco 715 circular dichroism (CD) spectropolarimeter using a 0.1 cm cell. The system was purged with nitrogen at 50 L/min. Data acquisition parameters were as follows: range, 250–190 nm; sensitivity, 50 mdeg; resolution, 0.2 nm; bandwidth, 1.0 nm; response, 1 s; scan speed, 20 nm/min; and, number of accumulations, 10. After background subtraction, the spectra were analyzed by a linear combination fit (Program Jfit, B. Rupp, unpublished, available from http://www-structure.llnl.gov/cd) using reference data of Greenfield and Fasman (18).

Protein crystallization. Crystallization was performed using the hanging drop vapor diffusion method. Drops containing a mixture of 3-μL protein solution (5.5 mg/mL) and 3 μL of reservoir solution were

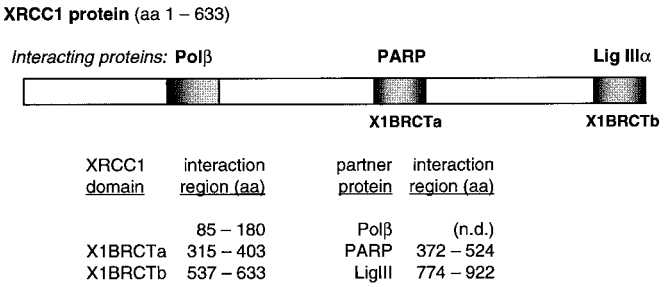

FIG. 1. Functional domains of XRCC1. Linear schematic indicating the regions of XRCC1 that interact with proteins implicated in the repair of DNA base damage: DNA polymerase β (Polβ) (10), PARP (9), and Lig IIIα (7; 8; and this study). n.d., not determined.

TABLE 1

Purification of Overexpressed X1BRCTb

Step	Protein (mg)	Yield (%)	Purification (fold)
Lysate	138	31	1.0
Macro Prep Q20 (Fraction II)	60	65	2.1
Superdex 75 (Fraction III)	29	98	3.2

Note. Yield and purification were determined by measuring the quantity of X1BRCTb in an SDS–polyacrylamide gel using densitometric scanning, compared to the total protein determined in each corresponding sample.

screened against a wide range of conditions at 4°C and room temperature. The conditions were chosen according to the output of the CRYSTOOL program (19; available from http://www-structure.llnl.gov/crystool/crystool.htm), which allows for a statistical sampling of a large parameter space. Crystals formed at room temperature within hours under a variety of conditions, which were further refined and finally reproducibly yielded diffraction quality crystals in 1.0 M ammonium sulfate, 0.1 M Tris–HCl, pH 6.7–7.1. Crystals of the Se-Met-containing protein were grown in the same buffer containing 5 mM 2-mercaptoethanol.

X-ray diffraction. For diffraction studies, crystals were harvested and briefly washed in crystallization buffer containing 30% (w/v) glycerol as a cryoprotectant, retrieved with a rayon cryoloop, and flash-cooled in liquid nitrogen. Crystals were maintained at near liquid nitrogen temperatures during data collection. Data from native crystals were collected on an ADSC dual multiwire detector system on a rotating Cu-anode X-ray generator (Rigaku RU200, $\lambda = 1.54178$ Å) and indexed and integrated using manufacturer-supplied software. Supplemental information about equipment and cryo procedures used are available from www-structure.llnl.gov. Data from the Se-Met-containing crystals were collected under cryo conditions on beamline 5.0.2 of the Macromolecular Crystallography Facility at the Advanced Light Source (ALS, Lawrence Berkeley National Laboratory, Berkeley, CA) using a 2 × 2 module ADSC CCD detector. Data were autoindexed, integrated, and merged using MOSFLM and SCALA of the CCP4 program suite (20).

RESULTS AND DISCUSSION

Purification of X1BRCTb. Because of the functional importance of the C-terminal region of XRCC1 in its interaction with Lig III (Fig. 1, and references therein) and the identification of this region as a putative structural domain (1, 2), we expressed and purified the human X1BRCTb polypeptide for biochemical and structural studies. The design of recombinant protein incorporates 101 amino acids encompassing the BRCTb domain, such that 5 native residues at the N-terminus and 4 at the C-terminus are outside the boundaries described strictly by homology (1). The resulting polypeptide has a calculated M_r of 11,928 and a pI of 4.6. Purified X1BRCTb was obtained by overexpression in *E. coli* and enrichment by anion-exchange and gel filtration chromatography. A two-step purification protocol was developed, including anion-exchange and gel filtration chromatography, that yielded 29 mg of highly purified X1BRCTb from 1 liter of bacterial culture. The protein is highly soluble, up to 27 mg/mL at pH 7 in our preparations, and the final X1BRCTb fraction was 98% pure as judged by densitometric evaluation of proteins separated by SDS–gel electrophoresis (Table 1 and Fig. 2).

During the process of refining the purification protocol, it was observed that the elution time of X1BRCTb on Superdex 75 was salt and protein concentration dependent. Increasing the salt concentration to at least

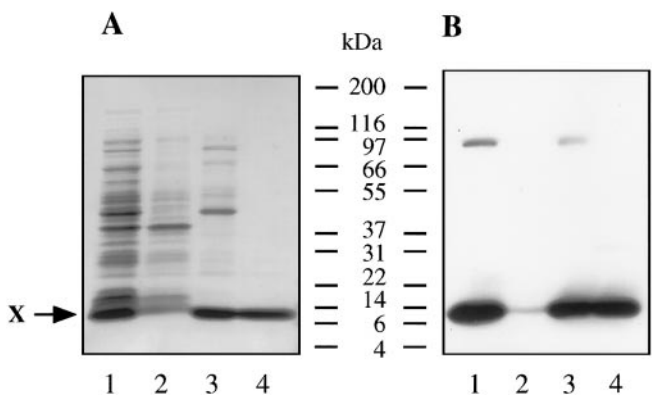

FIG. 2. Purification of X1BRCTb. (A) Coomassie-stained SDS–polyacrylamide gel of X1BRCTb purification fractions. Protein corresponding to 0.2 mL of the original bacterial culture was loaded in each lane. Lane 1, lysate (27.7 μg); lane 2, flowthrough from Q20 column (6.5 μg); lane 3, Fraction II from Q20 column (12.5 μg); lane 4, Fraction III from Superdex 75 column (5.8 μg). (B) Western blot of X1BRCTb purification fractions shown in A.

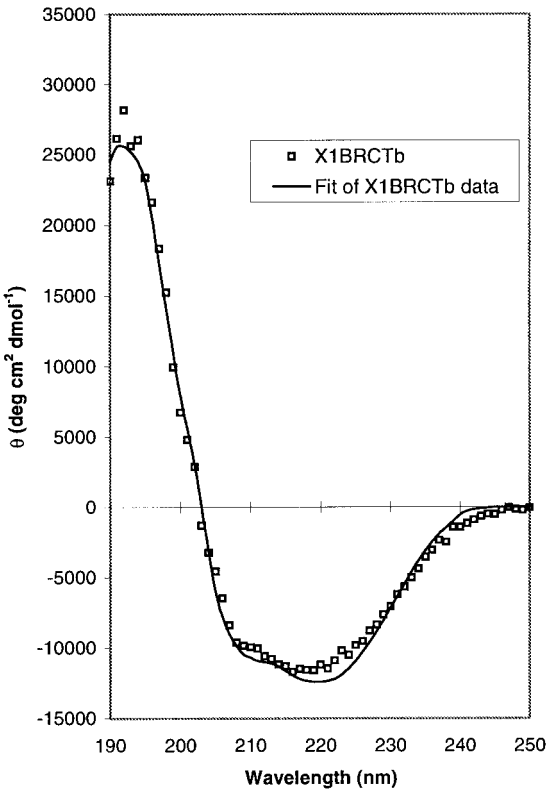

FIG. 3. CD spectrum of X1BRCTb. The sample contained 0.05 mg/mL purified X1BRCTb in 10 mM Na-phosphate buffer, pH 7.0. Experimental data represented as squares; theoretical curve fit, as a solid line.

0.5 M resulted in longer retention time and hence better separation from high molecular weight contaminants. This effect is likely due to oligomerization of X1BRCTb, occurring during either bacterial expression or chromatography, and the oligomers are apparently dissociated in higher salt concentrations. Based on M_r standards run under the same conditions as those used during purification, including 0.5 M salt, X1BRCTb was estimated at 30,000 Da, indicating that X1BRCTb is at least a dimer.

Solution conformation of X1BRCTb. Analysis of CD spectra of the purified X1BRCTb revealed a defined secondary structure containing approximately 64% of α-helix and 36% β-sheet (Fig. 3). The results from the CD analysis are consistent with secondary structure prediction of a consensus α-helical structure in BRCT domains and shorter, less well-defined β-sheet regions (1).

Functionality of X1BRCTb: Interaction with Lig IIIα. Having observed a folded structure by CD, we tested the native binding of X1BRCTb with Lig IIIα, the predominant form of Lig III (6), which contains a single, unusually short BRCT domain of 76 residues at the C-terminus (1, 2). The testis-specific Lig IIIβ form lacks this BRCT domain due to alternative mRNA splicing and does not bind XRCC1 (6, 7). Furthermore, these previous studies indicated that XRCC1 and Lig IIIα interact through their respective C-terminal regions and that the contact region in XRCC1 is within the BRCT domain of aa 537–633 (7, 8). In this study, we used a GST–affinity capture method to confirm that the overexpressed X1BRCTb domain binds preferentially to Lig IIIα *in vitro* (Fig. 4), as seen in previous affinity precipitation assays (7). In addition, the ease of crystal formation (see details below) of the purified protein strongly indicates that X1BRCTb domain is folded into a single conformation; i.e., there is no heterogeneity in the sample. These observations taken together indicate that the purified X1BRCTb likely retains the native structure in XRCC1 necessary for the interaction between the BRCT domains of XRCC1 and ligase III.

Crystallization and initial crystallographic characterization. Initial crystallization screening yielded X1BRCTb crystals under a variety of conditions. Further optimization led to reproducible growth of well-formed, bipyramidal, diffraction quality crystals (longest dimensions 0.5–0.7 mm) (Fig. 5). Crystals used for characterization formed in the presence of ammonium sulfate at neutral pH (Table 2). Diffraction data were collected at 125K and a complete data set could be

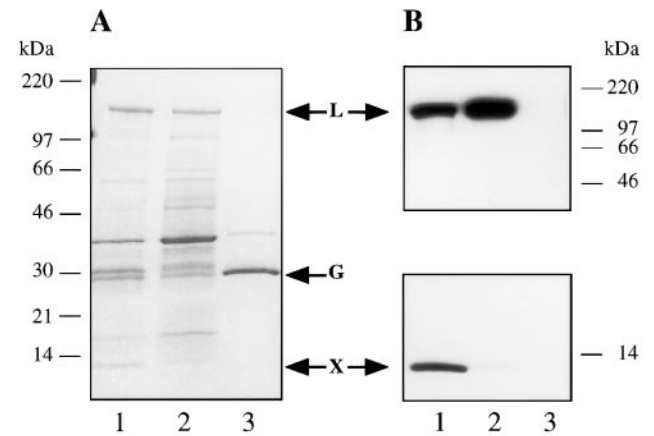

FIG. 4. Interaction of X1BRCTb domain with Lig IIIα. X1BRCTb was coexpressed in *E. coli* with either GST–Lig IIIα or β or GST alone, and resulting protein complexes were captured from the soluble lysates on glutathione–Sepharose as described under Materials and Methods. Proteins eluted from Sepharose were detected after SDS–gel electrophoresis (A) and immunoblotting (B). Lanes 1, X1BRCTb coexpressed with GST–Lig IIIα; lanes 2, X1BRCTb coexpressed with GST–Lig IIIβ; lanes 3, X1BRCTb coexpressed with the parental GST fusion protein. (A) Coomassie –blue-stained gel of samples containing equivalent amounts of GST fusion protein. (B) Immunoblot of bound proteins loaded in A. The nitrocellulose membrane was halved and probed with the appropriate antibodies.(Top) Lig III α and β proteins were detected using Lig III-specific antibodies. (Bottom) X1BRCTb was detected using XRCC1-specific antibodies.

FIG. 5. Crystals of X1BRCTb. Bipyramidal tetragonal crystals (0.7 mm largest dimension) diffracting to 2.85 Å. See Materials and Methods for growth conditions.

collected to 3.2 Å. The space group of the native crystals was determined to be $P4_12_12$ (or the enantiomorphic group $P4_32_12$), with unit cell dimensions $a = b = 100.53$ Å and $c = 105.85$ Å.

To enable MAD phasing of the diffraction data, Se-Met was incorporated into X1BRCTb during bacterial expression. The Se-Met-labeled protein crystallizes in the same tetragonal space group with nearly identical unit cell dimensions $a = 100.43$ Å and $c = 105.62$ Å (Table 2). MAD data were collected to 2.85 Å at the ALS at four wavelengths ($\lambda_1 = 0.9847$ Å, $\lambda_2 = 0.9851$ Å; $\lambda_3 = 1.0749$ Å, $\lambda_4 = 0.9297$ Å). λ_1 and λ_2 were selected to maximize f'' and f', respectively, as determined by an *in situ* EXAFS scan of the selenium K-edge of the mounted crystal. λ_3 and λ_4 correspond to two remote wavelengths on either side of the edge. MAD phasing of the data and structure determination is currently under way. From the unit cell dimensions and the molecular mass of the X1BRCTb polypeptide, we estimate that the unit cell contains four molecules in the asymmetric unit, yielding a Matthews coefficient of 3.05 $Å^3$/Da with a solvent content of 59.7%. Four molecules per asymmetric unit is consistent with the observed oligomerization of X1BRCTb.

During the review of our original manuscript, a structure of the XRCC1 BRCTb domain dimer was published by Zhang *et al.* (21). There are, however, several differences between the crystals reported in their study and ours. Zhang *et al.* found their crystals to be in the trigonal space group $P3_121$, whereas our crystals are tetragonal $P4_12_12$ (or its enantiomorph $P4_32_12$), giving rise to a considerably different packing environment in the unit cells. The presence of additional residues in our peptide (C-terminal DLPVP and N-terminal VPQA) potentially affects the packing in the crystals. In particular, the N-terminal inclusion of residues DLPVP in our construct is in close vicinity of the contact helices proposed by Zhang *et al.* and may influence the dimer contact conformations. The C-terminal modification may also induce different molecular packing due to changed intermolecular contacts.

Our native protein diffracts to considerably higher resolution than the selenomethionine crystals used for refinement of the published structure. Both the crystals in Zhang's report and the crystals in ours show rather large unit cells and similar high degrees of hydration, which, in both cases, appear related to the limited resolution of the diffraction data obtained.

In conclusion, we report the characterization and crystallization of the C-terminal BRCT domain of XRCC1. The X1BRCTb polypeptide isolated after overexpression in *E. coli* has a mostly helical structure (by CD), appears to be functional in specific protein–protein interactions, and readily forms crystals. X-ray diffraction data are of sufficient quality to pursue the crystal structure determination. Although a crystal structure has already been reported for X1BRCTb, our protein preparation crystallizes in a different space group from that reported by Zhang *et al.* Determination of the structure from a different crystal form will allow us to assess whether protein–protein contacts observed in the published dimer structure represent

TABLE 2

Crystallization Conditions (Room Temperature) and Data Collection Statistics for X1BRCTb Crystals

Crystal	Native	Se-Met
Crystallization conditions		
Buffer (Tris–HCl)	100 mM, pH 6.9	100 mM, pH 6.9
Precipitant (ammonium sulfate)	1 M	1 M
Additive (2-mercaptoethanol)	None	5 mM
Data collection statistics		
Space group[a]	$P4_12_12$	$P4_12_12$
a (Å)	100.53	100.43
c (Å)	105.85	105.62
d_{min} (Å)[b]	3.2	2.85
Observations (no.)	105,944	72,561
Unique reflections (no.)	26,022	13,640
Completeness (%)	98.9	70.0
R_{merge} (%)[c]	8.7	5.6
$\langle I/\sigma_{(I)}\rangle$	4.3	8.8
R_{ano} (%)[d]	n/a	2.6
Matthews Coefficient V_M ($Å^3$/Da)	3.05	
Solvent content (%)	59.7	
Molecules per asymmetric unit	4	

[a] Indistinguishable from its enantiomorphic space group $P4_32_12$ based on diffraction intensities alone.

[b] d_{min}, the smallest d-spacing for which reflections were measured.

[c] $R_{merge} = \Sigma_i(\Sigma_j|I_{ij} - \langle I_i\rangle|)/\Sigma_i\langle I_i\rangle$; I_{ij} is the scaled intensity of the jth observation of each unique reflection i and $\langle I_i\rangle$ is the mean value.

[d] $R_{ano} = \Sigma(|I^+ - I^-|)/\Sigma(I^+ + I^-)$, I^+ and I^- are intensities of corresponding Friedel mates. Wavelength selected ($\lambda_1 = 0.9847$ Å) maximizes anomalous (Bijvoet) differences.

the true conformation of the proposed recognition sites or are influenced by crystal packing. Knowledge gained from the structure of the BRCTb domain of XRCC1 will likely provide insight into the function of the many other BRCT domains in independent protein–protein interactions and moreover in DNA repair or other central biological processes.

ACKNOWLEDGMENTS

The authors are grateful to Drs. Brent Segelke, Thomas Earnest, and Mark Knapp for assistance with synchrotron data collection; Dr. Alan Tomkinson for GST-Lig III expression constructs and Lig III-specific antibodies; and Drs. Brent Segelke and David M. Wilson, III, for critical comments on the manuscript. This research was performed under the auspices of the U.S. DOE by LLNL under Contract W-7405-ENG-48 and was partly funded by NIH Grant CA76116 to M.P.T.

REFERENCES

1. Bork, P., Hofmann, K., Bucher, P., Neuwald, A. F., Altschul, S. F., and Koonin, E. V. (1997) A superfamily of conserved domains in DNA damage-responsive cell cycle checkpoint proteins. *FASEB J.* **11,** 68–76.
2. Callebaut, I., and Mornon, J. P. (1997) From BRCA1 to RAP1: A widespread BRCT module closely associated with DNA repair. *FEBS Lett.* **400,** 25–30.
3. Koonin, E. V., Altschul, S. F., and Bork, P. (1996) Functional motifs. *Nature Genet.* **13,** 266–268.
4. Caldecott, K. W., Tucker, J. D., and Thompson, L. H. (1992) Construction of human *XRCC1* minigenes that fully correct the CHO DNA repair mutant EM9. *Nucleic Acids Res.* **20,** 4575–4579.
5. Shen, M. R., Zdzienicka, M. Z., Mohrenweiser, H. W., Thompson, L. H., and Thelen, M. P. (1998) Mutations in hamster single-strand break repair gene *XRCC1* causing defective DNA repair. *Nucleic Acids Res.* **26,** 1032–1037.
6. Mackey, Z. B., Ramos, W., Levin, D. S., Walter, C. A., McCarrey, J. R., and Tomkinson, A. E. (1997) An alternative splicing event which occurs in mouse pachytene spermatocytes generates a form of DNA ligase III with distinct biochemical properties that may function in meiotic recombination. *Mol. Cell. Biol.* **17,** 989–998.
7. Nash, R. A., Caldecott, K. W., Barnes, D. E., and Lindahl, T. (1997) XRCC1 protein interacts with one of two distinct forms of DNA ligase III. *Biochemistry* **36,** 5207–5211.
8. Taylor, R. M., Wickstead, B., Cronin, S., and Caldecott, K. (1998) Role of a BRCT domain in the interaction of DNA ligase III-α with the DNA repair protein XRCC1. *Curr. Biol.* **8,** 877–880.
9. Masson, M., Niedergang, C., Schreiber, V., Muller, S., Ménissier-de Murcia, J., and de Murcia, G. (1998) XRCC1 is specifically associated with poly(ADP-ribose)polymerase and negatively regulates its activity following DNA damage. *Mol. Cell. Biol.* **18,** 3563–3571.
10. Kubota, Y., Nash, R. A., Klungland, A., Schar, P., Barnes, D. E., and Lindahl, T. (1996) Reconstitution of DNA base excision-repair with purified human proteins: Interaction between DNA polymerase β and the XRCC1 protein. *EMBO J.* **15,** 6662–6670.
11. Saka, Y., Esashi, F., Matsusaka, T., Mochida, S., and Yanagida, M. (1997) Damage and replication checkpoint control in fission yeast is ensured by interactions of Crb2, a protein with BRCT motif, with Cut5 and Chk1. *Genes Dev.* **11,** 3387–3400.
12. Critchlow, S. E., Bowater, R. P., and Jackson, S. P. (1997) Mammalian DNA double-strand break repair protein XRCC4 interacts with DNA ligase IV. *Curr. Biol.* **7,** 588–598.
13. Iwabuchi, K., Bartel, P. L., Li, B., Marraccino, R., and Fields, S. (1994) Two cellular proteins that bind to wild-type but not mutant p53. *Proc. Natl. Acad. Sci. USA* **91,** 6098–6102.
14. Yamane, K., Kawabata, M., and Tsuruo, T. (1997) A DNA-topoisomerase-II binding protein with eight repeating regions similar to DNA-repair enzymes and to a cell-cycle regulator. *Eur. J. Biochem.* **250,** 794–799.
15. Friedman, L. S., Ostermeyer, E. A., Szabo, C. S., Dowd, P., Lynch, E. D., Rowell, S. E., and King, M-C. (1994) Confirmation of *BRCA1* by analysis of germline mutations linked to breast and ovarian cancer in ten families. *Nature Genet.* **8,** 399–404.
16. Cormack, G. (1997) Unit 8.5 *In* "Current Protocols in Molecular Biology" (Ausubel, F. M., *et al.*, Eds.), Wiley, New York.
17. LeMaster, D. M., and Richards, F. M. (1985) ^{1}H-^{15}N heteronuclear NMR studies of *Escherichia coli* thioredoxin in samples isotopically labeled by residue type. *Biochemistry* **24,** 7263–7268.
18. Greenfield, N., and Fasman, G. D. (1969) Computed circular dichroism spectra for the evaluation of protein conformation. *Biochemistry* **8,** 4108–4116.
19. Segelke, B. W. (1995) Ph.D. dissertation, University of California, San Diego.
20. CCP4 (1994) Collaborative Computing Project No. 4: A suite of programs for protein crystallography. *Acta Crystallogr. D* **50,** 760–763.
21. Zhang, X., Moréra, S., Bates, P. A., Whitehead, P. C., Coffer, A. I., Hainbucher, K., Nash, R. A., Sternberg, M. J. E., Lindahl, T., and Freemont, P. S. (1998) Structure of an XRCC1 BRCT domain: A new protein–protein interaction module. *EMBO J.* **21,** 6404–6411.